Climate Projections of salt-wedge intrusions in a Po river branch (Northern Adriatic Sea)

Sahameddin M. Kurdistani,[1] Giorgia Verri,[1]* Nadia Pinardi,[2] Giovanni Coppini,[1] Dario Conte[1]

[1]Centro Euro-Mediterraneo sui Cambiamenti Climatici, CMCC, Lecce 73100, Italy.

[2] Alma Mater Studiorum - Università di Bologna, Department of Physics and Astronomy, Bologna 40126, Italy

Corresponding author: Giorgia Verri (giorgia.verri@cmcc.it)

Key Points:

- Climate projections for a salt-wedge estuary show a strong seasonality in the foreseen increase of both the salt wedge intrusion length and the outflowing salinity
- A two-layer estuary box model is provided to work as an impact tool for coastal environmental projections

Abstract

Estuaries are the transitional systems between the riverine freshwaters and the ocean salt water. Increasing salt-wedge intrusions are mentioned as one of the major impacts of climate change in coastal areas. We propose a new methodology to predict salt wedge intrusions with an intermediate complexity model, so-called Estuarine Box Model (EBM), that allows to use hydrology and ocean climate scenarios to predict salt wedge intrusions. We apply this methodology to the Goro branch of the Po river flowing into the Northern Adriatic Sea. A 30 years' period (1982-2011) is used to train and test the EBM that is then used to project the salt wedge in the (2021-2050) time period under the RCP8.5 emission scenario. The numerical results show that in the (2021-2050) period, the Po di Goro salt wedge intrusion length will increase by 15% on an annual basis (up to 50% in summertime) and the outflowing salinity will increase 9% on annual basis (up to 35% in summer). Finally, a statistical estimation of the extreme values of salt wedge and outflowing salinity shows return periods of 10 years for extremes twice the present mean values. It means that a 16 Km of salt-wedge intrusion, and outgoing salinity about 28 psu are highly expected as an extreme event with 10 years return period

Plain Language Summary

Salt wedge climate projections for one branch of the Po river Delta show a seasonality in the increase of the salt wedge intrusion length up to 50% in summer time considering the RCP8.5 climate scenario

1 Introduction

River salt-wedge intrusions are important threats to the quality of inland waters (*1*). Regionally downscaled climate change scenarios do not properly consider the river salt-wedge intrusions because their grid spacing cannot represent the estuary geometry and they do not involve a proper river-seawater coupling. If we want to gain insight on the trends of salt wedge intrusions along the river estuaries, we need to couple regional climate models with intermediate complexity models that can represent the estuarine overturning circulation and mixing processes as a result of the competition between the upstream riverine freshwater discharge and the ocean waters at the river mouths.

Recent literature on salt-wedge intrusion (SWI) projections has considered the changes in the upstream river flow and the sea level rise (SLR) under different climate change scenarios (*2*, *3*). The overall result is that the river discharge changes are expected to affect the SWI more than the SLR. A source of uncertainty is represented by the use of global or at most regional scale SLR (*4*) without considering the coastal effects probably because no regional downscaled scenario reaches the resolution required to resolve the local SLR (*5, 6*).

An additional challenge is the computational resources required to perform long term numerical experiments with very high-resolution hydrology and ocean models to resolve the estuary geometry. For this reason, the SWI response to climate change has been evaluated by means of synthetic experiments and/or annual mean experiments with upstream river runoff and ocean water inflow averaged over multidecadal time windows representing the present and future climate (*2*, *3*). There is a need to have an impact model tool, capable to run many decades, with inputs from the hydrological changes upstream the estuary and the ocean salt water changes at the estuary mouth.

In the past 10 years, other studies have simulated the temporal variability of the SWI length. (*7*) provided an empirical estimate of this length scale in river-dominated estuaries and the EBM presented in (*8*) followed this formulation. The current study uses a novel, intermediate complexity model, the so-called CMCC EBM model (*9*, *10*), which solves the estuarine water exchange by two conservation equations for volume and salt averaged over the diurnal tidal cycle. The EBM has been applied to the Goro branch of the Po river which is a river-dominated estuary and flows into the micro-tidal Adriatic Sea (Fig. 1).

The main aim of this study is to show how to predict climate change impacts on SWI and outflowing estuarine-water salinity with an intermediate complexity model, a new salt intrusion impact model, encompassing the main estuarine dynamics processes.

The question asked is: is the salt-wedge changing in the future climate scenarios and why? To what degree the estuarine dynamics is dominated by changes in the upstream river discharge?

In section 2 we describe the modeling strategy and the forcing data used to perform the climate experiments. Section 3 presents the results on the salt-wedge intrusion scenario and the changes in outflowing salinity. Moreover, a statistical estimation of the extreme values is provided. Conclusions are in section 4. Finally we briefly describe the CMCC EBM model in Appendix A and the Bootstrap method used for the statistical analysis in Appendix B.

2 Methodology

2.1 Modeling Strategy

The use of intermediate complexity models in climate change coastal impact studies is important because the earth system climate models do not consider the complex coastal geometry and the very local processes while mitigation and adaptation plan actions concentrate on very localized areas of high social and economic impact. This is the case of estuarine areas where the freshwaters meet the saltwater and eventually give rise to SWI phenomena and river plumes on the offshore area of the estuary that might affect primary, secondary and tertiary marine production (*11*, *12*) in addition to groundwater salt contamination. The more recent earth system models are still not able to properly couple model components at the land-sea interface (*13,4,5,6*) and in order to study the interactions between river waters and the sea it is necessary to use intermediate complexity models such as the Estuarine Box Model of this study.

The two unknowns of our study are the SWI length and the salinity of the outflowing waters: the first has obvious implications for the salinization of inland waters already mentioned and the second affects the coastal circulation and dynamics off the river mouths, i.e. the river plume, as well as the large-scale circulation *(14*).

2.2 River forcing: historical data and climate projections

The scenario of the Po discharge has been predicted by (*15*) using a hydrological model forced by a regional atmospheric model (*16*) nested in a global earth system climate model (*17*). *(15)* computed the RCP8.5 scenario projections for the Po at Pontelagoscuro (Fig.1) which is located right upstream of the Po delta river branches. For the historical (1982 – 2011) period, the Po river discharge was taken from observations at Pontelagoscuro hydrometer station. Figure 2a depicts daily discharge values observed during the (1982 – 2011) period having a time mean discharge of 1482 m^3/s while Fig. 2b shows the predicted discharge for Po at Pontelagoscuro for the scenario period (2021–2050) amounting to 1205 m^3/s. Thus the mean annual discharge of the Po river is reduced in the future period by approximately 23% with respect to the present conditions. We estimate the Goro branch of the Po river receives about 13% of the discharge at Pontelagoscuro (10) so in all our calculations we will use the upstream Po di Goro discharge value as the Po discharge at Pontelagoscuro scaled by 0.13.

2.3 Ocean forcing: historical data and climate projections

The EBM considers a two-layer flow in the estuary averaged over the estuarine horizontal areas. The lower layer inflowing salinity, S_{ll}, and volume flux, Q_{ll}, for both the past state and the future scenario period were taken from the ocean component of a regional climate model (*18*). The Q_{ll} shows an average value of 3.3 m^3/s in the historical period while 3.1 m^3/s for the scenario period, corresponding to a decrease of about 6%. The S_{ll} values show mean values of 35.3 psu for the historical period and 35.6 psu for the scenario period indicating a 1% increase.

The volume flux due to the flood tides Q_{tidef} is taken from the OTPS astronomical tidal model in its regional configuration over the Mediterranean Sea with 1/30-degree horizontal resolution (*19*). The mean tidal flow, extracted during the diurnal flood tide phases and averaged over 30 years, amounts to 18.6 m^3/s for the historical period and 18.7 m^3/s for the scenario period, given the short period considered for astronomical parameters to change. Thus all the ocean lateral boundary conditions here considered change relatively little with respect to the river discharge and this strongly affect the salt-wedge projections.

3 Results

3.1 Salt-wedge intrusion projections

Using the CMCC-EBM model, the SWI length L_x and the outflowing upper layer salinity S_{ul} have been computed for both historical and scenario periods. Figure 3 shows the values of Lx for the historical period (1982-2011) with the long-term average value of Lx

= 8.1 Km. For the scenario period (2021– 2050) Lx increases by 1.2 km, i.e. a 15% increase over the present condition values.

Similarly, the outflowing upper layer salinity is higher as shown in Figure 4(a, b) where the salinity at the river mouth will increase of 1.1 psu in the mid-term scenario with respect to the present climate (corresponding to a 9% increase on annual basis).

The comparison of the seasonal daily mean values over the two 30 years' periods for L_x and S_{ul} is shown in Fig. 5(a, b). The (2021-2050) projections show a larger increase of L_x during summer, arriving to a 40% increase in the July-August period with respect to present conditions. For the outflowing upper layer salinity, we see an increase from 20 to 25 psu during the summer months. In the (2020-2050) period we expect the salinity at river mouth will rise up to 35% in summer while a decrease is foreseen over November-January.

In conclusions we argue that the river discharge is the driver of SWI length and the salinity changes at the river mouth, neglecting the local SLR trends at the river mouth that are not available for this region. The other forcing changes, such as the inflowing lower layer salinity and volume flux are negligible with respect to upstream discharge changes. Nevertheless, even knowing the changes upstream and downstream of the river, it will be impossible to calculate the exact changes in SWI length without the CMCC-EBM which encompasses all the necessary physical processes.

3.2 Extreme values estimation

In addition to the projection of mean changes with respect to the present climate, it is important to define the probability of extreme events in terms of return periods. The Peak Over Threshold (POT) (*20*) method has been used to generate the input dataset of the extreme values of SWI lengths and outflowing upper layer salinity. One of the key choices in the POT method is to decide a threshold value. For the extreme values, the threshold has been considered as the minimum value of the yearly maximum values during the historical period (1982-2011) which produces the threshold values of 12 Km for L_x and 23 psu for S_{ul}.

Literature shows that the PDF of positive definite atmospheric and ocean variables are skewed and heavy-tailed (*21*, *22*). Figure 6(a, b) shows that the frequencies of occurrence of the daily values of L_x and S_{ul} follow a Weibull probability density function PDF (*23*) for both parameters. The *Bootstrap percentile method* (*24,25,26*) has been applied to compute the confidence intervals of the parameters β and σ as the "shape" and "scale" parameters of the Weibull PDF for the data of L_x and S_{ul}. Details are in the Appendix B.

The probability curves of the extreme values of the L_x and S_{ul} as function of their return periods $\boldsymbol{T}$ along with the upper and lower 95% confidence intervals are shown in Fig. 7a and Fig. 7b respectively. The return period is by definition $\boldsymbol{T = \frac{1}{1-P_{x\leq x_{max}}}}$ where $\boldsymbol{P_{x\leq x_{max}}}$

is the Weibull cumulative distribution function representing the probability that the variable x (L_x and S_{ul} in this work) is less than or equal to the selected threshold $\boldsymbol{x_{max}}$.

The salt wedge values of 16 km and 20 km registered during the historical period (when the mean SWI length is found to be equal to 8.1 km) are expected with 10 and 100 years return periods respectively. Red points in Fig. 7a are the projected values of L_x by EBM model for the scenario period (2021-2050). In the projections L_x values of 20 km will have a shorter return period of about 60 years.

Moreover, the river mouth salinity values of 28 psu and 34 psu registered during the historical period (when the mean outflowing salinity at river mouth is found to be equal to 12.9 psu) are also expected to occur with 10 and 100 years return periods (Fig. 7b). Red points in Fig. 7b are the projected values of S_{ul} by EBM model for the scenario period (2021-2050) and the 34 psu values will have a shorter return period of about 50 years. showing reliable predictions inside the upper-lower 95% confidence intervals for all the return periods.

Overall the hazard estimation shorter short return periods of the extreme values of outflowing salinity and SWI length: return periods of 10 years (high occurrence probability) are found for extremes twice the present mean values. Moreover, the EBM projections show even shorter return periods with respect to the extreme values of L_x *and* S_{ul} computed during the historical period.

4 Conclusions

An intermediate complexity estuarine box model, so-called CMCC-EBM, has been used for the first time as an impact model to study SWI and outflowing salinity in rivers for present and future climate conditions. The CMCC-EBM couples the hydrology and the shelf ocean waters from general circulation models. In this way the simulations we carried out include the 2way feedback between riverine and marine waters by solving the estuarine water exchange mechanism.

This study shows that, for a river-dominated estuary flowing into a micro-tidal sea, the river discharge reduction is the main factor affecting the increase of the salt-wedge length and the river outflowing salinity. The numerical findings for the Po di Goro river branch depict an average lengthening of the SWI in the (2021-2050) period equal to 1.2 km (meaning a 15% increase) and an increase of the river outflowing salinity of 1.1 psu (corresponding to a 9% increase). This increase has a large seasonal cycle, the projections showing a sharp increase in summer time for the SWI length and the salinity up to 40-50% of the present state values.

The extreme values of SWI and outflowing salinity computed during the historical period are found to have relatively short return periods of about 10 years (high occurrence probability) for extremes twice the present mean values . SWI maximum values such as

20 km, have return periods of 100 years for the historical period and about 60 years in the projected climate.

Overall the projected changes in the SWI length of the Po di Goro branch provide a valuable piece of information for adaptation policies since it is already clear that this region is facing increasing salinization of inland waters. Furthermore, it is known that a change of several psu in river outflowing salinity has the potential of changing the ocean circulation and dynamics from coastal to large scales (*14*). For all these reasons above, the CMCC-EBM intermediate complexity model used here could be a valuable impact tool for coastal environmental projections and impact studies.

Appendix A: The Estuarine Box Model

The CMCC EBM (*9*, *10*), (http://www.estuaryboxmodel.org) is based on the assumption of a two-layer flow dynamics in the estuary. The continuity equation and the salinity advection-diffusion equation are integrated in each layer and across the horizontal dimensions of the estuary, its length and width (see Fig. A1). This produces conservation equations for the volume flux and the salt flux supposed to be uniform in each layer. The two resulting equations are:

$$\boldsymbol{Q_{ul} = Q_{river} + Q_{ll} + H\,L_y u_{tidef}} \quad (1)$$

$$\boldsymbol{S_{ul} = S_{ul}Q_{ul} + \overline{S}\,HL_y u_{tidef} + K_{SH}HL_y \frac{\overline{S}}{L_x}} \quad (2)$$

where H, L_y, L_x the estuary depth, width and length respectively. The subscripts "*ul*" and "*ll*" refer to the upper and lower estuary layers respectively, $\boldsymbol{u_{tidef}}$ is the barotropic velocity corresponding to the flood tide phase, $\boldsymbol{\overline{S}}$ is the depth averaged ocean salinity and $K_{SH} = C_k L_y u_{tidef}$, the horizontal eddy diffusivity where C_k is the non-dimensional eddy diffusivity coefficient representative of the estuary stratification and described in *(10)* by a parametric equation using the dimensional analysis. The lateral ocean input fields at the estuary mouth are: Q_{ll}, S_{ll}, $\overline{\boldsymbol{S}}$ and $\boldsymbol{u_{tidef}}$. The river volume flux Q_{river} has to be provided at the estuary head, i.e. at the last section along the river network moving in the

downstream direction where the salinity is still equal to zero on multi-year average conditions.

The estuary length in CMCC-EBM is considered to represent the Salt-Wedge Intrusion (SWI) length which changes dynamically following a parametric equation developed by (10) for the Goro branch of the Po river:

$$\boldsymbol{L_x = 10\, H\, F_r^{-0.3} \left(\frac{\rho_{ll}}{\rho_0}\right)^{40} \left(\frac{H}{h}\right)^{-4.6} \left(\frac{Q_{tidef}}{Q_{river}}\right)^{0.3} \left(\frac{Q_{ll}}{Q_{river}}\right)^{-0.01}} \qquad (3)$$

where F_r is the river Froude number, F_r is the tidal Froude number, $Q_{tidef} = L_y\, H\, \boldsymbol{u_{tidef}}$, ρ_0=1000 kgm^{-3} is the river freshwater density, $\rho_{ll}= \rho_0\,(1+k_s\, S_{ll})$ with the haline contraction coefficient taken to be constant and equal to k_s=7.7 10^{-4} psu^{-1} (*10*).

These three equations will give estimates $\boldsymbol{of}$ the outflowing volume flux Q_{ul}, the salinity S_{ul} and the SWI length L_x which we propose as an impact model to be interfaced with the climate projected input fields for Q_{river} and Q_{ll}, S_{ll}, $\overline{\boldsymbol{S}}$ and $\boldsymbol{u_{tidef}}$.

Appendix B: The confidence levels of the extreme values

As it has been explained in the main body of the paper, the Peak Over Threshold (POT) method has been employed to define the probability of extreme events observed during the historical range in terms of their return periods. The POT datasets of the extreme values of SWI lengths and outflowing salinity are the historical daily values which exceed a threshold defined as the minimum value of the yearly maximum values, i.e. 12km and 23psu respectively.

Figure 6(a, b) shows that the frequencies of occurrence of the POT daily values of both L_x and S_{ul} follow a Weibull probability density function PDF (*25*).

The *Bootstrap percentile method* (*26*) has been applied to compute the confidence intervals of the "shape" and "scale" parameters of the Weibull distribution for extreme L_x and S_{ul} shown in Figure 7.

The Bootstrap method (*24*, *25*) is a resampling technique to perform statistical inference directly from the data. The bootstrap is typically computed with a randomized algorithm.

The practitioner randomly generates B new datasets (i.e. the Bootstrap samples) by drawing randomly from the original dataset consisting of N values (i.e. the first guess).

The first guess of Bootstrap percentile is represented by the POT daily values of Lx and S_{ul} respectively. The number of resampling is chosen B = 1000.

Considering β and σ as the "shape" and "scale" parameters of the first guess, $\boldsymbol{\beta_j^*}$ and $\boldsymbol{\sigma_j^*}$ are the "shape" and "scale" parameters of the Bootstrap samples (j = 1 to 1000). The Bootstrap percentile method determines the standardized variable $\boldsymbol{z^*_{\beta_j}} = \frac{\boldsymbol{\beta}}{\boldsymbol{\beta_j^*}}$ and $\boldsymbol{z^*_{\sigma_j}} = \frac{\boldsymbol{\sigma}}{\boldsymbol{\sigma_j^*}}$.

In this way, the appropriate limiting values of the standardized parameters may be directly read from the list of their B estimates ranked in descending order of magnitude (j from 1 to 1000).

Following Meeker et al. (2017) (*26*), in order to identify the bounding values of β and σ corresponding to the 95% confidence interval, we compute $B*(\alpha/2)$ = 1000* (0.05/2) = 25 which means that in the ranked values of $\boldsymbol{z^*_{\beta_j}}$ and $\boldsymbol{z^*_{\sigma_j}}$ the 25th value is the upper percentile value, i.e. $\boldsymbol{z^*_{\beta_{upper}}}$ and $\boldsymbol{z^*_{\sigma_{upper}}}$ respectively. Similarly, $B*(1-(\alpha/2))$ = 1000 (1- (0.05/2)) = 975 means that the 975th value is the lower percentile value $\boldsymbol{z^*_{\beta_{lower}}}$ and $\boldsymbol{z^*_{\sigma_{lower}}}$ respectively.

The upper and lower values di β and σ corresponding to the 95% confidence interval are then computed from the upper level and lower values of $\boldsymbol{z^*_{\beta}}$ and $\boldsymbol{z^*_{\sigma}}$ as it follows:

$$\left[\boldsymbol{\beta_{lower}}, \boldsymbol{\beta_{upper}}\right] = \left[\boldsymbol{z^*_{\beta_{lower}}} * \boldsymbol{\beta}, \boldsymbol{z^*_{\beta_{upper}}} * \boldsymbol{\beta}\right] \tag{5}$$

$$\left[\boldsymbol{\sigma_{lower}}, \boldsymbol{\sigma_{upper}}\right] = \left[\boldsymbol{z^*_{\sigma_{lower}}} * \boldsymbol{\sigma}, \boldsymbol{z^*_{\sigma_{upper}}} * \boldsymbol{\sigma}\right] \tag{6}$$

Finding these upper and lower values of the Weibull distribution parameters, makes it possible to have the probability curves of the prediction of the extreme values of L_x and S_{ul} shown in Fig. 7a and Fig. 7b along with the 95% confidence intervals.

Acknowledgments

The authors are grateful to the Regional Agency for Prevention, Environment and Energy of Emilia-Romagna (Arpae) for providing the salinity observations at the Manufatto gauge and the Po river runoff data at the Pontelagoscuro station.
This research was funded by the OPERANDUM project and the EU Copernicus Marine Environment Monitoring Service projects of the Mediterranean Sea Monitoring and Forecasting (n. 74-351 CMEMS-MFC-MED-N). OPERANDUM project has received funding from the European Union's Horizon 2020 research and innovation program under grant agreement No. 776848.

Open Research

The CMCC EBM is free and open software under the terms of the LGPL license, distributed from its web page (http://www.estuaryboxmodel.org) where a Test Case on Po di Goro estuary with the model inputs and outputs are accessible and interoperable. The data archiving of CMCC EBM historical simulations and future projections here discussed is underway on the webpage; in the meantime, the EBM input data and results are included as supplementary material.
The observational datasets used in this study for the calibration and validation of the CMCC EBM are publicly available. The observations of salinity at the Po di Goro mouth (Manufatto gauge) and the Po river runoff at the Pontelagoscuro station are findable through the Arpae repository and accessible at the Arpae webapp (https://simc.arpae.it/dext3r).

References

1. T.R. Green, "Linking Climate Change and Groundwater" in Integrated Groundwater Management: Concepts, Approaches and Challenges. (Springer International Publishing, 2016), pp. 97-141.
2. A. Tsz Yeung Leung, J. Stronach, J. Matthieu, Modelling Behaviour of the Salt Wedge in the Fraser River and Its Relationship with Climate and Man-Made Changes. *Journal of Marine Science and Engineering*. **6**(4), 130: 1-29 (2018).
3. D. Bellafiore, C. Ferrarin, F. Maicu, G. Manfe, G. Lorenzetti, G. Umgiesser, L. Zaggia, A.V. Levinson, Saltwater intrusion in a Mediterranean delta under a changing climate. *Journal f Geophysical Research: Oceans*. **126**(2), (2021).
4. Adloff, F., Jordà, G., Somot, S., Sevault, F., Arsouze, T., Meyssignac, B., ... & Planton, S.. Improving sea level simulation in Mediterranean regional climate models. *Climate dynamics*, **51**(3), 1167-1178, (2018)
5. Somot, S., Ruti, P., Ahrens, B., Coppola, E., Jordà, G., Sannino, G., & Solmon, F. Editorial for the Med-CORDEX special issue. *Climate Dynamics*, **51**(3), 771-777, (2018).
6. Torresan, S., Gallina, V., Gualdi, S., Bellafiore, D., Umgiesser, G., Carniel, S., ... Critto, A. Assessment of climate change impacts in the North Adriatic coastal area. Part I: a multi-model chain for the definition of climate change hazard scenarios. *Water*, **11**(6), 1157, (2019).
7. P. MacCready, W. R. Geyer, Advances in Estuarine Physics. *Annu. Rev. Marine. Sci.* **2**(1), 35-58 (2010).
8. Q. Sun, M. M. Whitney, F. O. Bryan, Y. H. Tseng, A box model for representing estuarine physical processes in Earth system models. *Ocean Modelling*, **112**, 139-153 (2017).
9. G. Verri, N. Pinardi, F. Bryan, Y. Tseng, G. Coppini, E. Clementi, A box model to represent estuarine dynamics in mesoscale resolution ocean models. *Ocean Modeling*. **148**, 1-14 (2020).

10. G. Verri, S.M. Kurdistani, G. Coppini, A. Valentini, Recent advances of a box model to represent the estuarine dynamics: time-variable estuary length and eddy diffusivity. *Journal of Advances in Modeling Earth Systems (JAMES)*. **13**(4), 1-16 (2021).
11. K. Watanabe, A. Kasai, E.S. Antonio, K. Suzuki, M. Ueno, Y. Yamashita, Influence of salt-wedge intrusion on ecological processes at lower trophic levels in the Yura Estuary, Japan. *Estuarine, Coastal and Shelf Science*. **139**, 67-77 (2014).
12. N.C. James, L. van Niekerk, A.K. Whitfield, W.M. Potts, A. Götz, A.W. Paterson, Effects of climate change on South African estuaries and associated fish species. *Climate Research*. **57**, 233-248 (2013).
13. M. Claussen, L. Mysak, A. Weaver, Earth system models of intermediate complexity: closing the gap in the spectrum of climate system models. *Climate Dynamics*. **18**, 579-586 (2002).
14. G. Verri, N. Pinardi, P. Oddo, S.A. Ciliberti, G. Coppini, River runoff influences on the Central Mediterranean Overturning Circulation. *Climate Dynamics*. **50**(5-6), 1675–1703 (2018).
15. R. Vezzoli, P. Mercogliano, S. Pecora, A. Zollo, C. Cacciamani, Hydrological simulation of Po River (North Italy) discharge under climate change scenarios using the RCM COSMO-CLM. *Science of the Total Environment*. **521**(2), 346-358 (2015).
16. E. Bucchignani, M. Montesarchio, A. Zollo, P. Mercogliano, Regional climate simulations with COSMO-CLM over the Mediterranean area. *Advances in Climate Science*. 338-351 (2014).
17. E. Scoccimarro, S. Gualdi, A. Bellucci, A. Sanna, P.G. Fogli, E. Manzini, M. Vichi, P. Oddo, A. Navarra, Effects of Tropical Cyclones on Ocean Heat Transport in a High-Resolution Coupled General Circulation Model. *Journal of Climate*. **24**(6), 4368-4384 (2011).
18. L. Cavicchia,S. Gualdi, A. Sanna, P. Oddo, The regional ocean-atmosphere coupled model COSMO-NEMO MFS. *CMCC Research Paper*. Issue RP0254, (2015).
19. D. Egbert, S.Y. Erofeeva, Efficient inverse modeling of barotropic ocean tides. *Journal of Atmospheric and Oceanic Technology*. **19**(2), 183-204 (2002).
20. M.R. Leadbetter, On a basis for 'Peaks over Threshold' modeling. Statistics and Probability Letters. **12**, 357-362 (1991).
21. A.A. Sepp Neves, N. inardi, A. Navarra, F. Trotta, A General Methodology for Beached Oil Spill Hazard Mapping. *Frontiers in Marine Science*. **7**, 1-10 (2020).
22. P.D. Sardeshmukh, G.P. Compo, Need for Caution in Interpreting Extreme Weather Statistics. *Journal of Climate*. **28**, 9166-9187 (2015).
23. W. Weibull, A Statistical Distribution Function of Wide Applicability. *ASME Journal of Applied Mechanics* - Transactions of the American Society of Mechanical Engineers., 293-297 (1951).
24. B. Efron, Bootstrap Method: Another Look at the Jackknife. *The annals of Statistics*. **9**, 1-26 (1979).
25. B. Efron, R.J. Tibshirani, "An Introduction to the Bootstrap" (Chapman and Hall, 1994), pp. 1-436.
26. W.Q. Meeker, G.J. Hahn, L.A. Escobar, "Statistical Intervals" (JOHN WILEY and SONS, 2017), pp. 1-578.
27. G.I. Barenblatt, "Dimensional analysis" (CRC Press, 1987).

Figures

Fig. 1. The Goro branch of the Po river. It has a river-dominated estuary and flows into the micro-tidal Adriatic Sea.

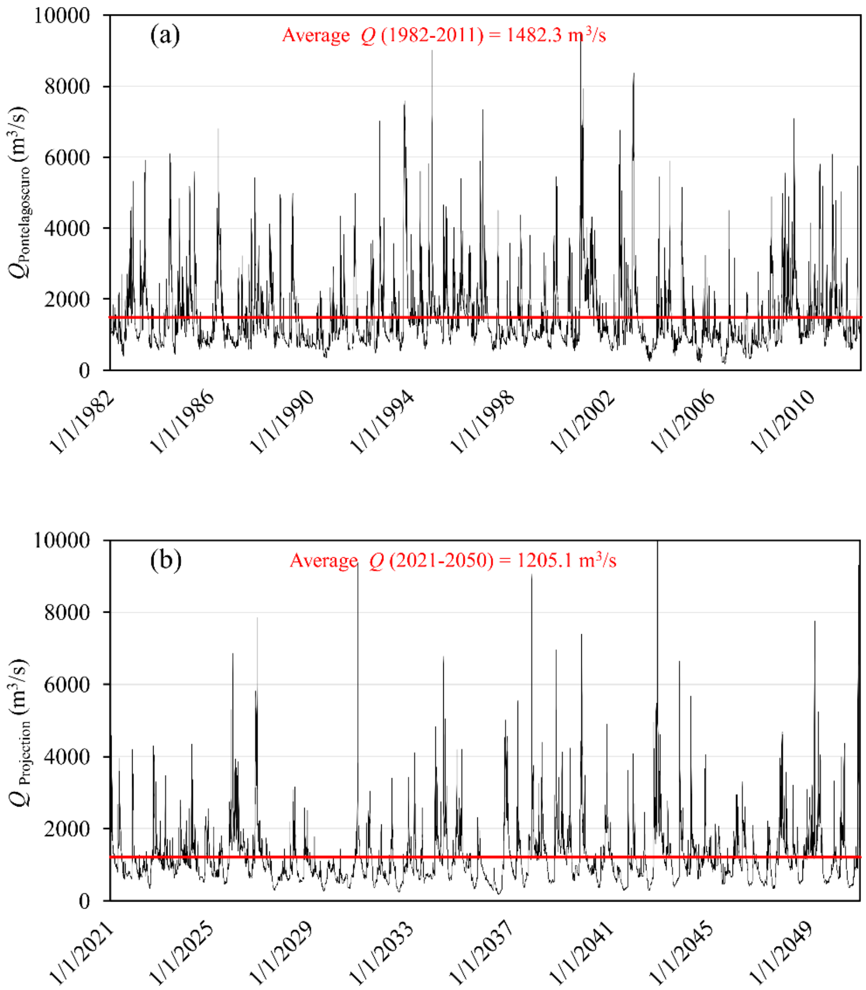

Fig. 2. Pontelagoscuro hydrometry station. (**A**) observed discharge values during (1982 – 2011), (**B**) predicted discharge values for the scenario period (2021–2050).

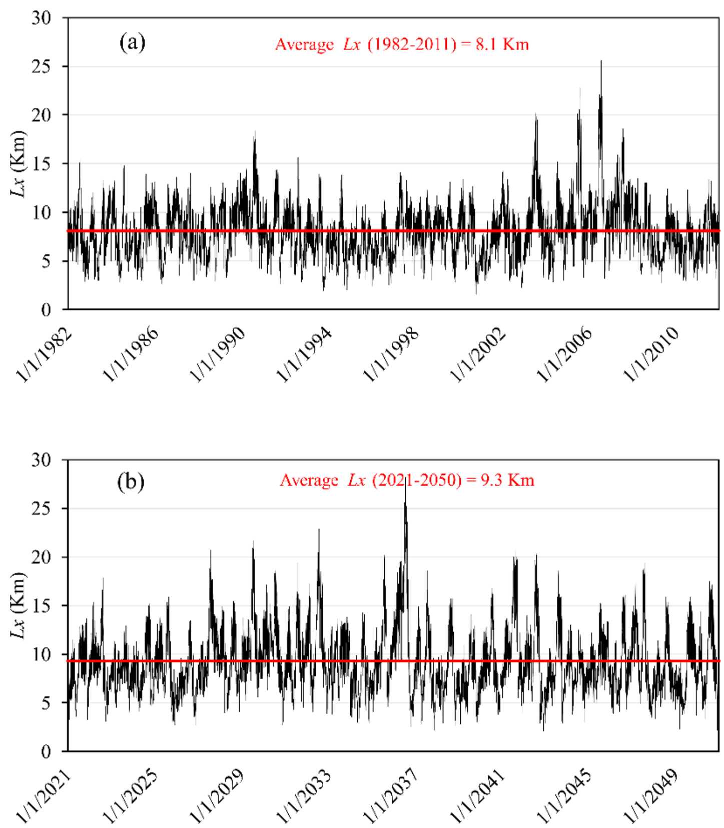

Fig. 3. Salt-wedge intrusion (EBM model). (**A**) historical period (1982-2011), (**B**) scenario period (2021–2050).

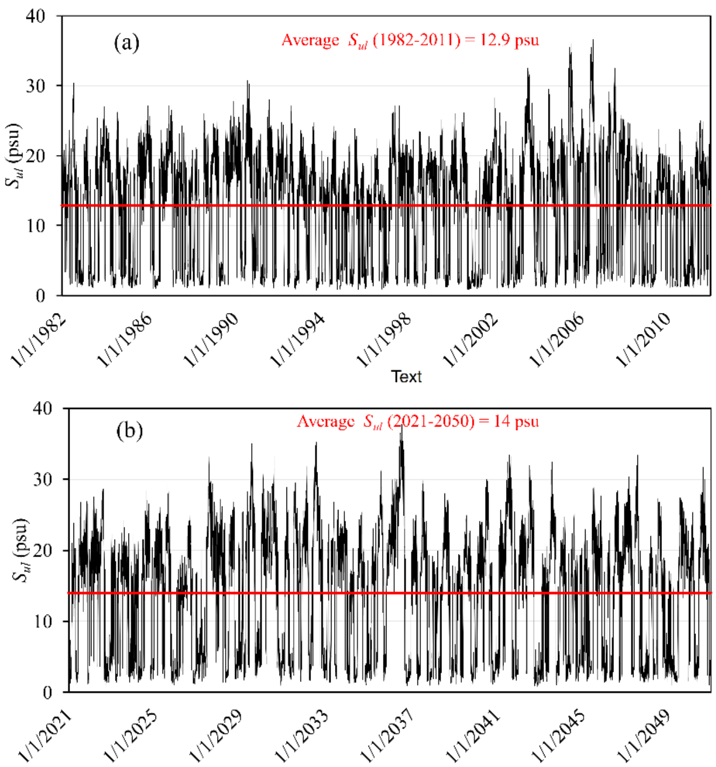

Fig. 4. Outflowing salinity (EBM model). (**A**) historical period (1982-2011), (**B**) scenario period (2021–2050).

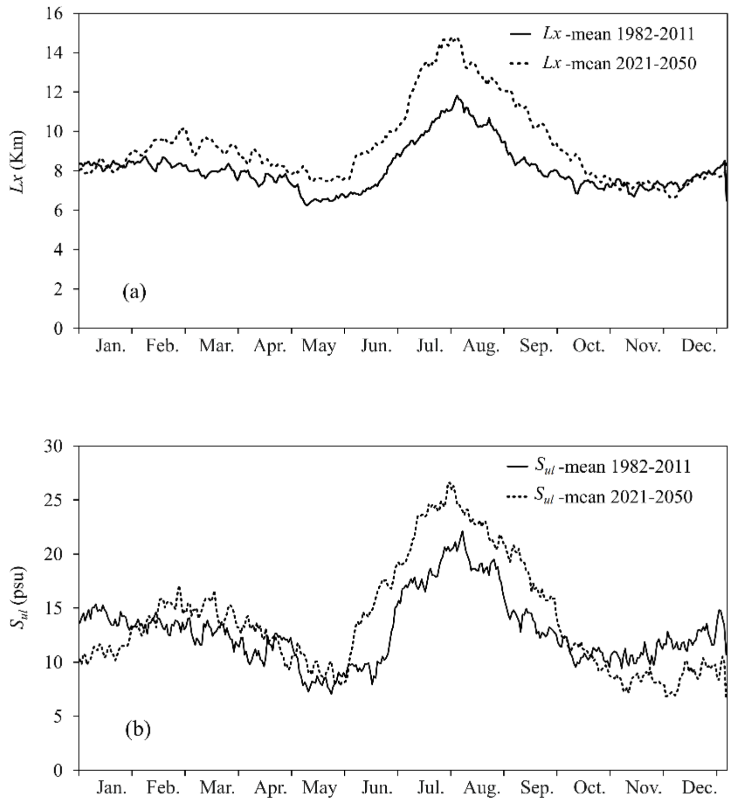

Fig. 5. Seasonal cycle of daily mean values (EBM model). (**A**) Salt-wedge intrusion, (**B**) Outflowing salinity.

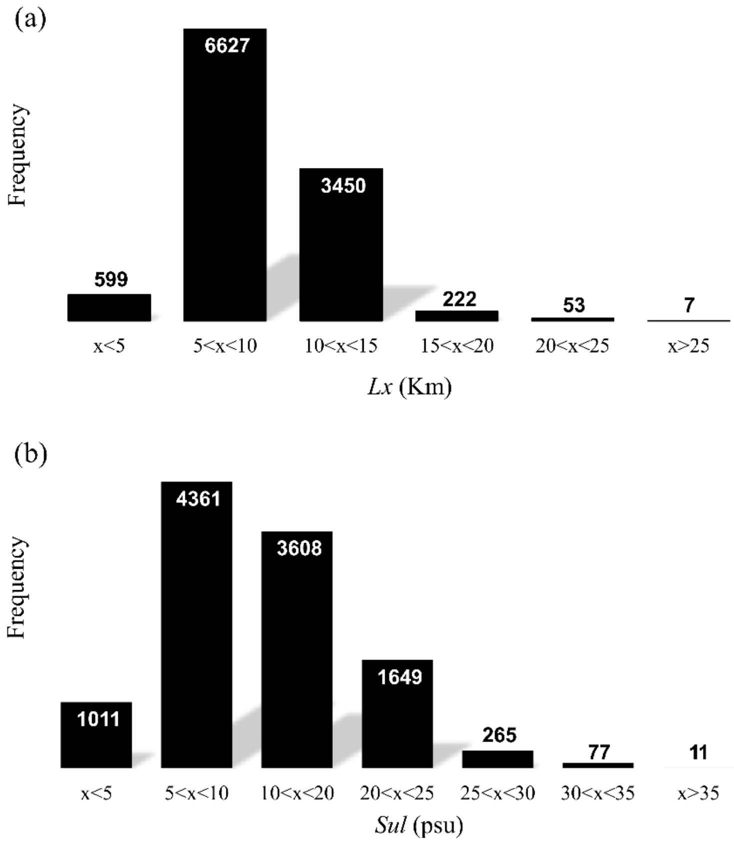

Fig. 6. Frequencies of occurrence of daily values. (**A**) Salt-wedge intrusion, (**B**) Outflowing salinity.

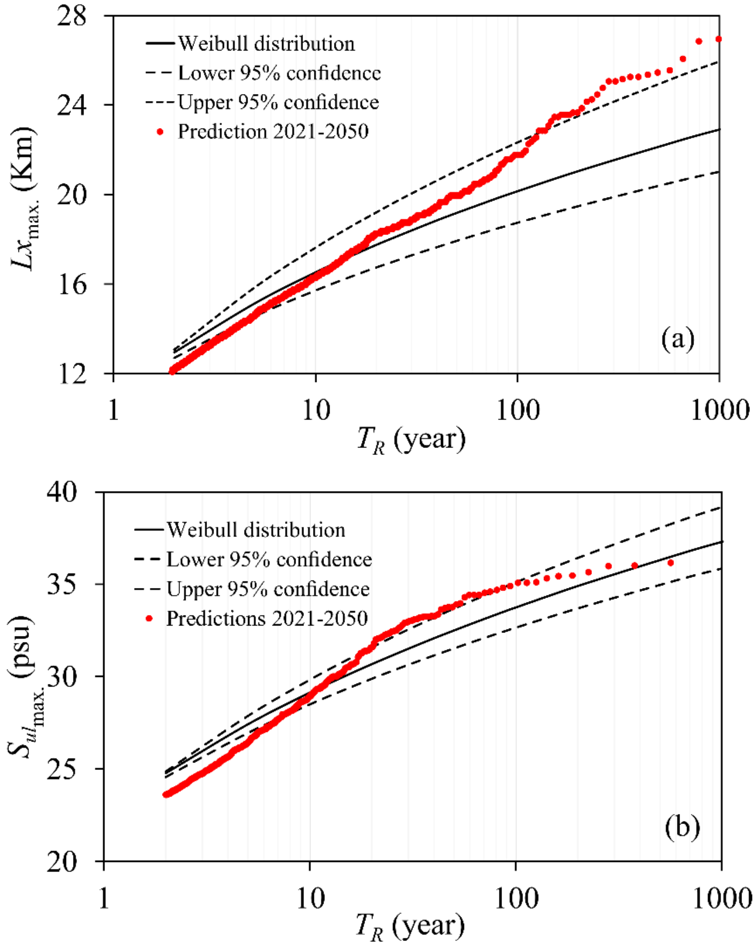

Fig. 7. Probability curves with upper-lower 95% confidence intervals. (**A**) Compared with the predicted values of L_x for the scenario period (2021-2050), (**B**) Compared with the predicted values of the outflowing salinity for the scenario period (2021-2050).

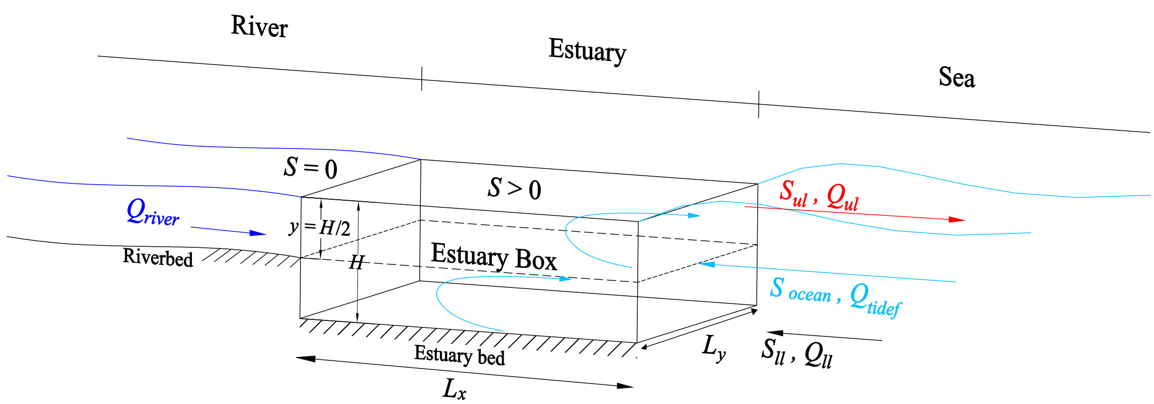

Fig. A1 Sketch of the CMCC EBM model. Black arrows stand for input variables coming from coupled models or observational datasets, red arrows indicate the unknowns solved by the EBM. The pairs of blue arrows represent the tidal mixing. The model source code is open and free and it is available here: http://www.estuaryboxmodel.org